Electronic Supplementary Information for full paper submitted for publication in Dalton Transactions

Reconstruction and catalytic activity of hybrid Pd(100)/(111) monolayer over γ-Al_2O_3(100) in CH_4, H_2O, and O_2 dissociation

A.A. Rybakov[a], S. Todorova[b], D.N. Trubnikov [a], A.V. Larin[a*]

[a]*Department of Chemistry, Moscow State University, GSP-2, Leninskie Gory, Moscow 119992, Russia*

[b]*Institute of Catalysis, Bulgarian Academy of Sciences, Acad. G. Bonchev St., Bldg 11, 1113 Sofia, Bulgaria*

TOTAL PAGES 26

TABLES 4

FIGURES 5

APPENDIXES 2

*) corresponding author: nasgo@yandex.ru

Part S1. Comparative charge analysis with Bader, Mulliken, and Löwdin schemes

A difference between the partition schemes of the obtained charges is the wider range of the Al charges with Mulliken or Löwdin scheme (around ~1 |*e*| compared to ~0.06 |*e*| for Bader charges) and the wider charge intervals for O within Bader scheme (around ~0.4 |*e*| compared to ~0.2 |*e*| for Mulliken ones). More importantly, different ranges of Pd charge variations are given which we would associate with Pd reactivity, *i.e.,* 0.60 |*e*| between the largest and smallest Bader Pd charges, third column (B) from the right of Table 2 and 0.33 |*e*| between the largest and smallest Mulliken or Löwdin Pd charges, second (M) and first (L) columns from the right, respectively, of Table 2.

We will compare below mostly Bader and Mulliken schemes (Table S2) because the Mulliken and Löwdin charges usually correlate rather accurately (Fig. S3e-h), especially for Pd (Fig. S3g) and Al (Fig. S3e). Unfortunately, insufficient number of two digits after comma in Lobster output for the charges does not allow to precisely evaluate an accuracy of the correlations that is clearly evident from the "steps" in Figs. S3b, f, h. The Bader scheme does not differentiate charge state of octahedral AlO_6 and $Al(OH)O_5$ atoms (if one Al-O bond is replaced by terminal Al-O(H)). A small reduction (~0.02 |*e*|) in tetrahedral AlO_4 position is calculated for the $Al(OH)_2O_2$ type after bond replacement by two terminal Al-O(H) (respective points in the ellipse shown by dotted circle in Fig. S3a) groups from the lower slab side (Fig. 1). A slightly larger charge reduction (~0.04 |*e*|) is obtained for those Al whose one Al-O bond is replaced by Pd-Al one (the upper 5-coordinated Al are in Pd-contact, shown by dashed circle in Fig. S3a). It is a questionable decrease owing to the higher O electronegativity (3.44 using Pauling scale[1]) compared to the one of Pd (2.2).[1] The Mulliken and Löwdin schemes differentiate separate groups of the Al charges which contact or do not (the octahedral are shown by dotted-dashed circle in Fig. S3a) with OH groups for both octahedral and tetrahedral Al atoms compared to Bader one. The charges of the octahedral and tetrahedral Al atoms are larger when Al-O(H) bond

replaces Al-O in opposite to the Bader changes. But the latter results in the high Bader Al charges within a narrow interval where variations do not agree with Mulliken's estimates while replacing Al-O(Al) by Al-O(H) group. If the Mulliken scheme predicts Al charge growth upon such a replacement (within the charge range limited by dotted-dashed circles, on the left side, and dotted circle, on the right side, in Fig. S3a), the Bader Al charges show an opposite reduction.

Part S2. Computational details

The scripts provided by the Transition State Tools for VASP were used to build the initial images for the climbing image nudged elastic band (cNEB) calculations. The energy cut-off was set to 500 eV. The Brillouin zone *k*-sampling was restricted to the Γ–point for the geometry optimization and transition state (TS) search *via* cNEB calculations. Spin polarized solution was considered for testing the basic Pd/(100)γ-Al_2O_3 model. Integral crystal orbital overlap populations (ICOOP) and Hamilton-weighted populations (ICOHP) (see part S3) were calculated with the Lobster code 3.2.0.[2] Vibrational frequencies were calculated using the finite difference method (0.015 Å atomic displacements) as implemented in VASP. For all reactions, the TS showed a single imaginary frequency corresponding to the reaction path. The figures of the 3D structure of the different models were drawn with MOLDRAW 2.0.[3] Reactions simulation videos (see ESI) were implemented using wxMacMolPlt.[4] GPU version of the VASP code[5,6] was massively used for geometry optimization.

For comparison of the barriers calculated at Pd multi-layer slab, the model of 5-layer Pd(100) slab grown at the same $Al_{36}O_{64}H_{16}$ model[7] was applied. In order to keep Pd(100) orientation whose presence was shown in the system Pd/γ-Al_2O_3[8] the growing was realized by the relaxation of 2-layer Pd(100) fragments superimposed at γ-Al_2O_3.[7,9] Such a procedure was repeated three times, then the sixth layer was deleted together with support and the lowest layer

was frozen.[9] The close DOS structures of the Pd atoms at the full 6-layer model (with the support) and of the shorten 5-layer one was shown earlier.[10]

Part S3. ICOOP and ICOHP occupations

Integral crystal orbital overlap occupations (ICOOP) (S1) or Hamilton-weighted occupations (ICOHP)[2] (S2) can be obtained *via* averaged COOP(E) or COHP(E) functions of energy (E), respectively, over projected density of states (the sum in the right hand side of eq. (S3)) up to Fermi energy ε_F over all j-populated bands using elements of population matrix ($S_{\mu,\mathbf{T},\nu,\mathbf{T'}}$) or Hamiltonian operator ($H_{\mu,\mathbf{T},\nu,\mathbf{T'}}$) between μ- and ν-atomic orbitals (AOs) centered at atoms A and B in unit cells shifted by vectors **T** and **T'**:

$$\mathrm{ICOOP}(\varepsilon_F) = \int^{\varepsilon F} \mathrm{COOP(E)dE} \qquad \text{(S1)}$$

$$\mathrm{ICOHP}(\varepsilon_F) = \int^{\varepsilon F} \mathrm{COHP(E)dE} \qquad \text{(S2)}$$

$$\mathrm{COOP(E)} = S_{\mu,\mathbf{T},\nu,\mathbf{T'}} \sum_{j,\mathbf{k}} C_{\mu,\mathbf{T},j}(\mathbf{k}) C_{\nu,\mathbf{T'},j}(\mathbf{k}) \delta(\varepsilon_j(\mathbf{k}) - E) \qquad \text{(S3)}$$

$$\mathrm{COHP(E)} = H_{\mu,\mathbf{T},\nu,\mathbf{T'}} \sum_{j,\mathbf{k}} f_j(\mathbf{k}) C_{\mu,\mathbf{T},j}(\mathbf{k}) C_{\nu,\mathbf{T'},j}(\mathbf{k}) \delta(\varepsilon_j(\mathbf{k}) - E) \qquad \text{(S4)}$$

where **k** are the vectors of reciprocal lattice, $C_{\mu,\mathbf{T},j}(\mathbf{k})$ is the coefficients of linear combinations of μ-AOs to represent crystal orbitals, $f_j(\mathbf{k})$ are occupation numbers. The expressions (S3, S4)[2] contain implicitly summation over all μ-ν-pairs between the atoms A and B. Simplifying, one could formulate that the largest ICOOP and –ICOHP values reveal a better stability of the selected bond A-B with the length *R* (Table 4).

If the occupation analysis was capable to confirm the better stabilization at the monolayer than at the Pd slab, the explanation of tiny differences between the reactions at Pd127 and Pd128 of the monolayer met some differences. The better stabilization and smaller dissociation barrier

$E^{\#}$ of 0.37 eV at Pd128 relative to that (0.67 eV) at Pd127 are not evident because –ICOHP(H18-O19)$_{0.37}$ > -ICOHP(H18-O19)$_{0.67}$ but ICOHP(H18-Pd127)$_{0.37}$ < -ICOHP(H18-Pd120)$_{0.67}$ (Table 4) where low indexes signify the barrier $E^{\#}$. Both respective relations in ICOOP terms show on a better TS stabilization and smaller dissociation barrier at Pd127 in opposite to the calculations.

References.

1 J. E. Huheey, *Inorganic chemistry; principles of structure and reactivity*, Harper & Row, New York, 1972.

2 S. Maintz, V. L. Deringer, A. L. Tchougréeff and R. Dronskowski, *Journal of Computational Chemistry*, 2016, **37**, 1030–1035.

3 P. Ugliengo, D. Viterbo and G. Chiari, *Zeitschrift für Kristallographie - Crystalline Materials*, 1993, **207**, 9–23.

4 B. M. Bode and M. S. Gordon, *Journal of Molecular Graphics and Modelling*, 1998, **16**, 133–138.

5 M. Hacene, A. Anciaux-Sedrakian, X. Rozanska, D. Klahr, T. Guignon and P. Fleurat-Lessard, *Journal of Computational Chemistry*, 2012, **33**, 2581–2589.

6 M. Hutchinson and M. Widom, *Computer Physics Communications*, 2012, **183**, 1422–1426.

7 A. A. Rybakov, I. A. Bryukhanov, S. Todorova, R. Velinova, A. Naydenov and A. V. Larin, *The Journal of Physical Chemistry C*, 2020, **124**, 605–615.

8 E. Garbowski, C. Feumi-Jantou, N. Mouaddib and M. Primet, *Applied Catalysis A, General*, 1994, **109**, 277–291.

9 A. A. Rybakov, I. A. Bryukhanov, A. V. Larin, S. Todorova and G. M. Zhidomirov, *Structural Chemistry*, 2019, **30**, 489–500.

10 A. A. Rybakov, I. A. Bryukhanov, A. V. Larin, S. Todorova, D. P. Vercauteren and G. M. Zhidomirov, *Catalysis Today*, 2020, **357**, 368–379.

Table S1. Bader (B), Mulliken (M), or Löwdin (L) charges (|e|) of the Pd atoms in the initial Pd(111) slabs deposited over γ-Al_2O_3(100) (18 deposited Pd atoms per cell). All data are obtained for spin-non-polarized solution. The "charge-charge" correlations *r* (the lowest row) of Mulliken and Löwdin charges are calculated relative to the Bader data in the "B" column. The correlation of the "B" column is calculated relative to the charges of the spin-non-polarized hybrid model ("SN" column of Table 2).

N	B	M	L
117	0.113	0.54	0.51
118	-0.196	0.44	0.41
119	0.333	0.75	0.72
120	0.114	0.49	0.47
121	-0.248	0.43	0.40
122	0.104	0.50	0.48
123	-0.155	0.43	0.40
124	-0.258	0.43	0.39
125	0.109	0.53	0.51
126	0.090	0.55	0.52
127	-0.260	0.42	0.39
128	0.325	0.75	0.72
129	0.119	0.51	0.48
130	-0.259	0.44	0.41
131	0.107	0.50	0.48
132	-0.146	0.43	0.40
133	-0.171	0.42	0.39
134	0.085	0.53	0.50
r	0.683	0.878	0.894
Q	-0.194	9.09	8.58

Table S2. Bader type charges of water (at both Pd_{18} and Pd_{20} monolayers), methane (case with the activation energy $E^{\#}$ = 0.19 eV in the lower row at Pd_{18}), and Pd atoms in the reagent (REA), transition state (TS) and product (PRO) for the $Al_{36}O_{64}H_{16}$ model (Fig. 1) and Pd_{90} slab (for $E^{\#}$ = 1.06 eV, see main text) optimized at the PBE-D3/PAW level. The Pd atom contacting with OH group after dissociation over $Al_{36}O_{64}H_{16}$ is shown by bold.

Atom	$E^{\#}$ = 0.37			$E^{\#}$ = 0.40		
	REA	TS	PRO	REA	TS	PRO
H17	0.618	0.595	0.601	0.614	0.585	0.601
H18	0.539	0.207	-0.056	0.638	0.215	-0.056
O19	-1.091	-0.952	-0.956	-1.150	-0.944	-0.956
Pd127	-0.008	0.041	0.347	0.125	0.004	0.347
Pd128	**0.337**	**0.358**	**0.358**	**0.347**	**0.366**	**0.358**
	$E^{\#}$ = 0.67			$E^{\#}$ = 1.06[a)]		
	REA	TS	PRO	REA	TS	PRO
H17	0.620	0.600	0.600	0.626	0.113	-0.036
H18	0.610	0.209	-0.050	0.614	0.574	0.589
O19	-1.139	-0.982	-0.959	-1.184	-0.967	-0.970
Pd127	**0.344**	**0.360**	**0.337**	**0.083**	**0.226**	**0.194**
Pd120	-0.302	-0.237	-0.158	-0.070	-0.028	0.004
	$E^{\#}$ = 0.19					
	REA	TS	PRO			
H17	0.052	0.060	0.077			
H18	0.093	0.080	0.059			
H19	0.021	0.106	-0.065			
H20	0.094	0.120	-0.004			
C21	-0.182	-0.264	-0.213			
Pd120	-0.250	-0.217	-0.162			
Pd127	0.243	0.206	0.209			

[a)] Pd71 and Pd64 atoms in the 5-layer Pd model; 1.09 eV at the PBE/PAW level

Table S3. Variations of Pd-Pd distances (R_i, i = 1 - 4, in Å) upon doubling unit cell size along OX axis (Case 2) relative to the initial ones (Case 1). The R_i, i = 1-3, distances are related to the monovacancy in the (111) fragment; R_4 corresponds to the monovacancy at the (111)/(100) boundary. The tested distances R_i are shown by the arrows in Fig. S2.

Case	R_1	R_2	R_3	R_4
1	4.084	4.078	5.393	3.770
2	4.127	4.128	5.473	3.794
ΔR_i	0.043	0.050	0.080	0.024

Table S4. Distances between water and Pd atoms in the reagent (REA), transition states (TS) and product (PRO) at Pd_{18} monolayers for the $Al_{36}O_{64}H_{16}$ model (Fig. 6) and Pd_{90} slab (for $E^{\#}$ = 1.06 eV, see main text) optimized at the PBE-D3/PAW level.

Atom	$E^{\#}$ = 0.37			$E^{\#}$ = 0.67		
	REA	TS	PRO	REA	TS	PRO
O19-H17	0.984	0.982	0.980	0.9853	0.983	0.980
O19-H18	1.048	1.544	3.133	0.9965	1.564	3.133
Pd127-O19	2.089	2.004	2.025	3.1916	3.003	2.025
Pd128-O19	2.844	2.875	2.102	2.1045	2.007	2.102
H18-Pd127	2.012	1.610	2.009	2.3864	2.089	2.009
H18-Pd120	3.774	3.428	1.700	2.534	1.676	1.700
H18-Pd126	3.859	3.492	1.795	3.0406	2.626	1.795
	$E^{\#}$ = 1.06					
	REA	TS	PRO			
O3-H2	0.9775	0.9797	0.9797			
O3-H1	0.9772	1.7695	2.9526			
Pd64-O3	2.3878	2.0399	2.1368			
Pd63-O3	3.6755	3.4124	2.0864			
H1-Pd64	2.7608	1.8682	1.6953			
H1-Pd71	3.1754	1.6416	1.6863			

Figure captions

Figure S1. The geometries of the (a) single Pd atom and (b) Pd_6, and (c-f) Pd_{13} clusters optimized at the $Al_{36}O_{64}H_{16}$ model using PBE-D3/PAW level without (a-c) and with (e-f) adsorbed CH_4. The Pd stabilization energies (eq. 1) are shown (eV/Pd) in Figures (a-c) according to the data from Table 1. The heats of CH_4 adsorption (eV) are shown in (d-f) at the PBE/PAW level. Pd charges are shown in (b). The atomic colors are given in pink (small spheres), red, magenta, and gray (large spheres) for H, O, Al, and Pd, respectively.

Figure S2. The geometry of the unit cell (UC) for $Al_{72}O_{128}H_{32}$ model with double lattice parameter along OX axis and Pd-Pd distances related to the monovacancy in the (111) fragment (R_i, i = 1-3), and the monovacancy at the (111)/(100) boundary (R_4). The R_i-variations between normal and double UCs are given in Table S2. The atomic colors are given in grey (small spheres), red, magenta, and gray (large spheres) for H, O, Al, and Pd, respectively.

Figure S3. Correlations between the Bader $q_B(X)$ and Mulliken $q_M(X)$ type charges (in *e*) of X = Al (a), O (b), Pd (c), and H (d) atoms, between the Mulliken $q_M(X)$ and Löwdin $q_L(X)$ type charges (in *e*) of X = Al (e), O (f), Pd (g), H (h) in $Pd_{18}Al_{36}O_{64}H_{16}$ model.

Figure S4. Final (a, c) or initial (b) geometries of the reagents (a) and products (b, c) of water dissociation optimized (a, c) at the PBE-D3/PAW level. The distances are commented in the text when given in the Figure. The arrows depict the initial (b) Pd-Al and final (c) Pd-O bonds. The atomic colors are given in gray (small spheres), red, magenta, and gray (large spheres) for H, O, Al, and Pd, respectively.

Figure S5. The transformation in the course (a $\rightarrow$ d) of the optimization of adsorbed water (a, c) at initial Pd(111) monolayer at the PBE-D3/PAW level. The unified two-vacancy (shown by two circles in (d)) is obtained instead of two isolated monovacancies (Fig. 2b, c). The shift down of the (H_2O)Pd128-Pd127-Pd120 chain (shown by ellipse in the (b)) is main result of the optimization (d). The atomic colors are given in gray (small spheres), red, magenta, and gray (large spheres) for H, O, Al, and Pd, respectively.

Figure S1

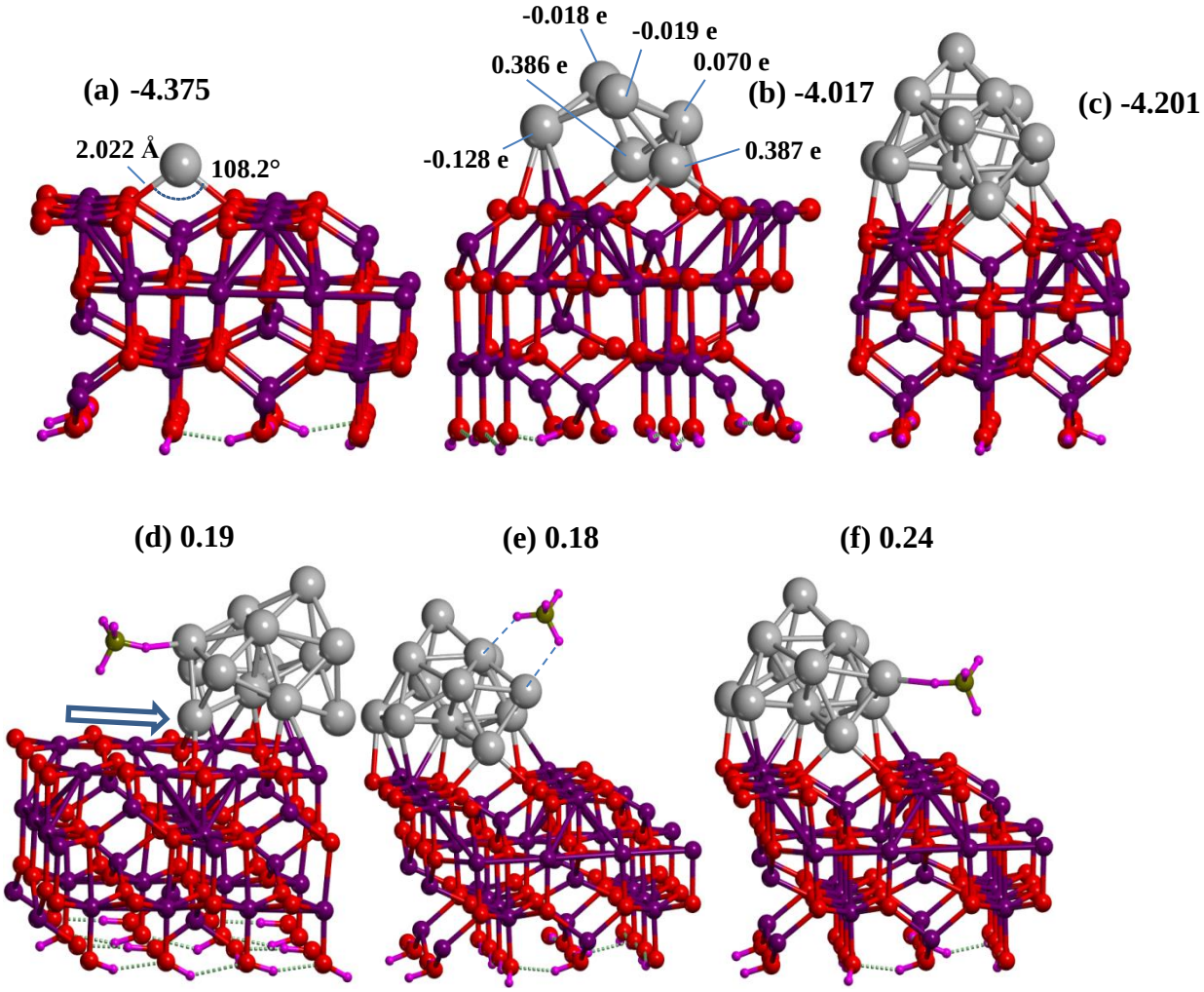
(a) -4.375
2.022 Å
108.2°
-0.018 e
-0.019 e
0.386 e
0.070 e
-0.128 e
0.387 e
(b) -4.017
(c) -4.201
(d) 0.19
(e) 0.18
(f) 0.24

Figure S2

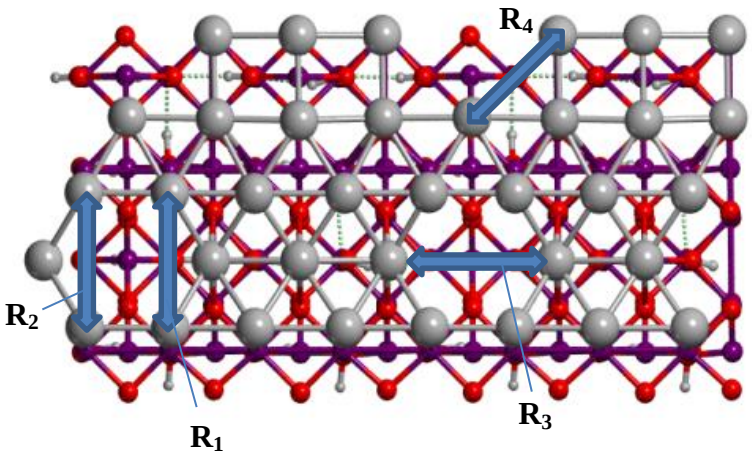

Figure S3

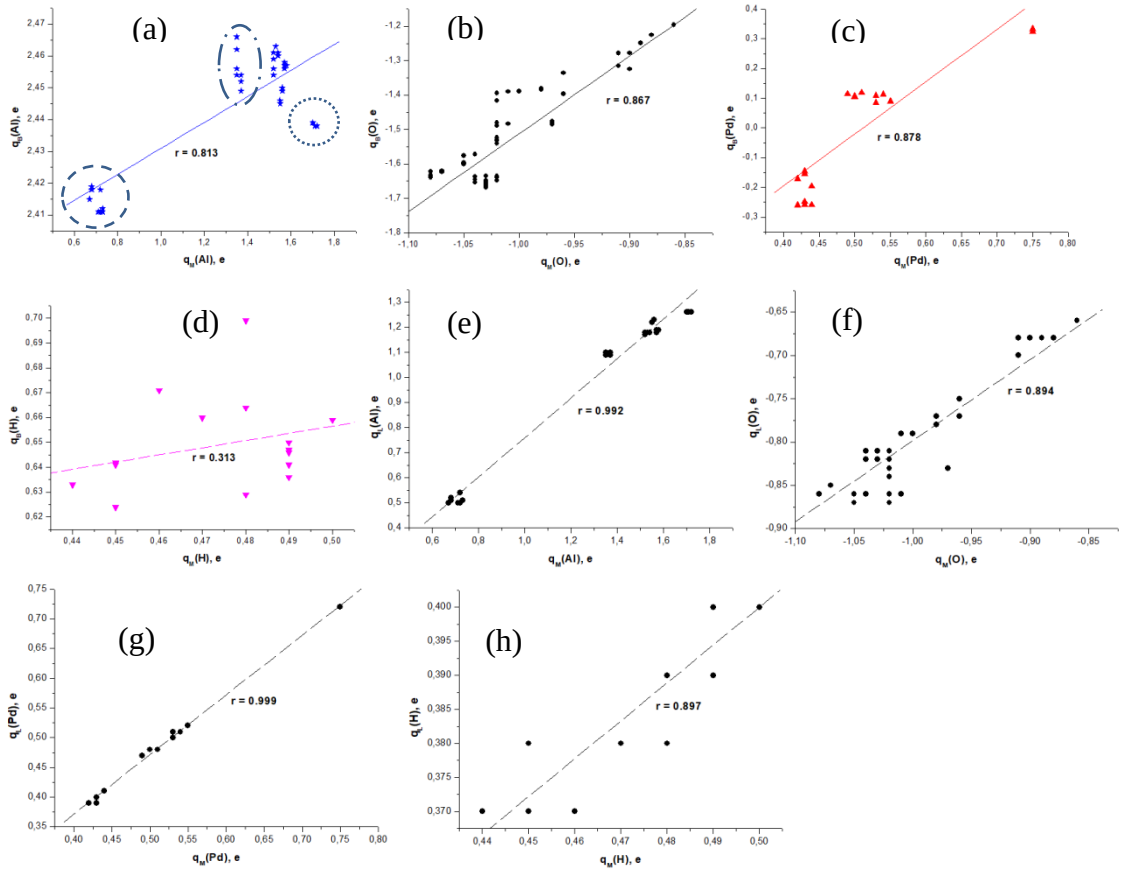
(a)
r = 0.813
q_M(Al), e
q_{Al}, e
(b)
r = 0.867
q_M(O), e
q_O, e
(c)
r = 0.878
q_M(Pd), e
q_{Pd}, e
(d)
r = 0.313
q_M(H), e
q_H, e
(e)
r = 0.992
q_M(Al), e
q_{Al}, e
(f)
r = 0.894
q_M(O), e
q_O, e
(g)
r = 0.999
q_M(Pd), e
q_{Pd}, e
(h)
r = 0.897
q_M(H), e
q_H, e

Figure S4

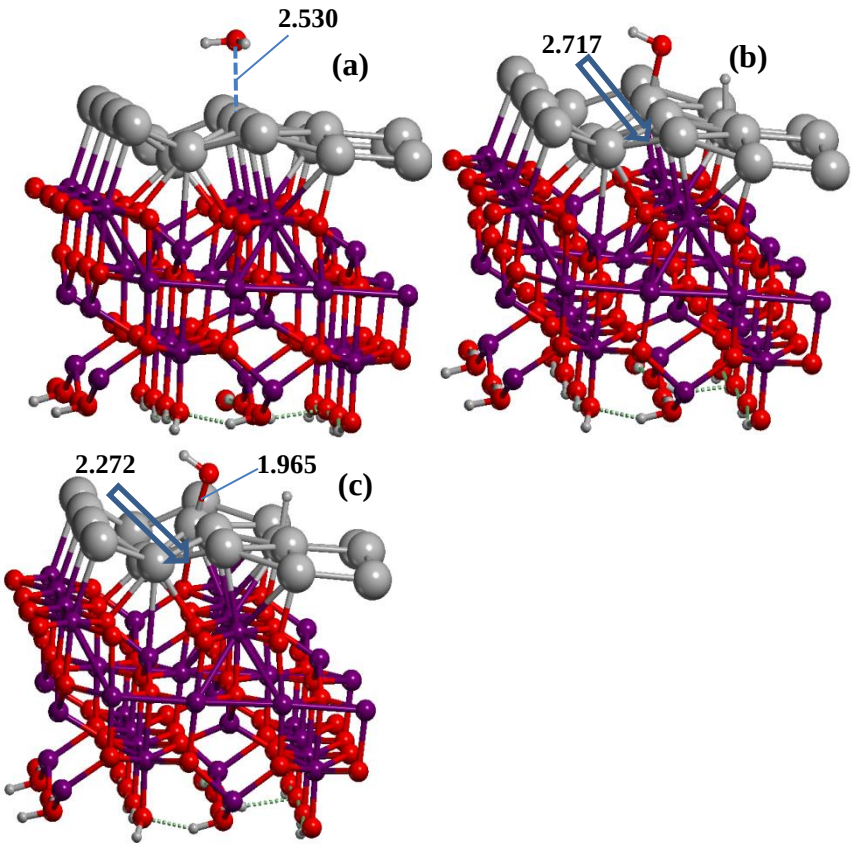

Figure S5

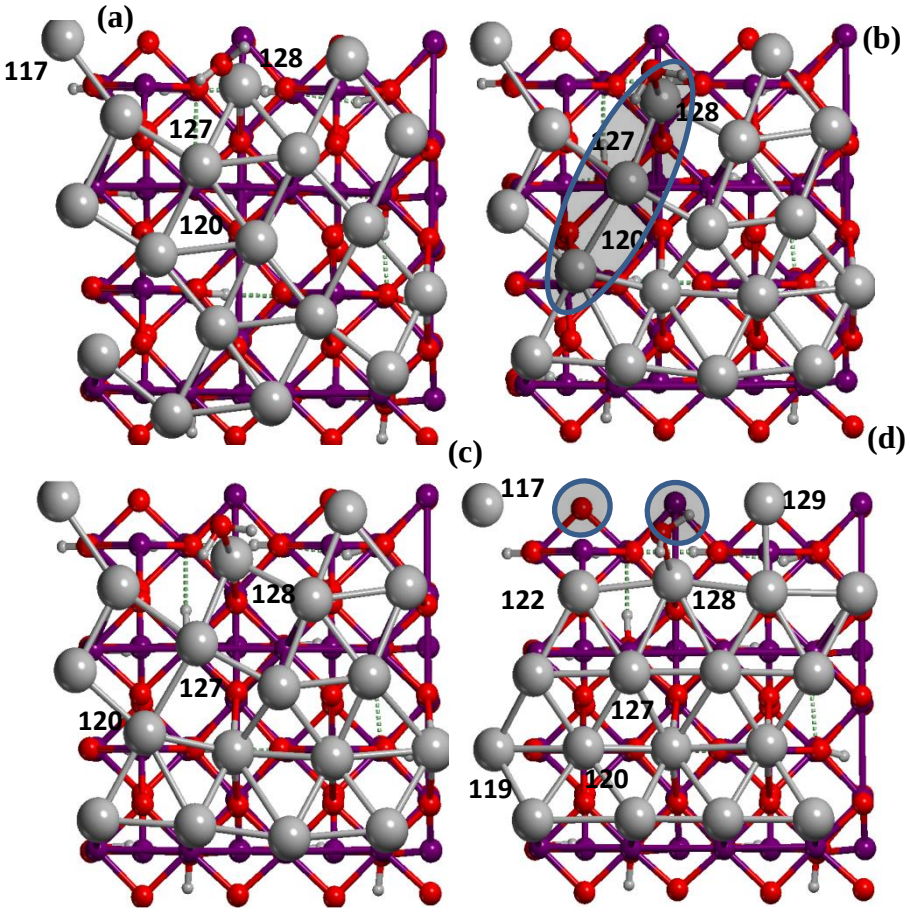
(a)
117
128
127
120
(b)
128
127
120
(c)
128
127
120
(d)
117
129
122
128
127
119
120

Appendix 1. The POSCAR file for the reagents of H_2O dissociation at Pd_{18}(1+1) monolayer with two isolated vacancies deposited over γ-Al_2O_3(100) (Fig. 6a) optimized at the PBE-D3/PAW level.

```
18   O 65   Al 36   Pd 18
 1.000000000
   11.217970     0.000000     0.000000
   -0.086360    11.216740     0.000000
    0.000000     0.000000    24.572338
   18     65     36     18
Selective
Cartesian
   2.27168832     6.90904948     0.50404605   F   F   F
   9.57579524     5.95842863     0.22909170   F   F   F
   7.87798454     7.08746022     0.50403255   F   F   F
   4.01639974     8.01688421     0.12601133   F   F   F
   4.06826525     0.37052309     0.19062090   F   F   F
   2.36322847     1.52587412     0.50973860   F   F   F
   9.65286251     0.31583286     0.24970387   F   F   F
   7.97273005     1.47428835     0.50495137   F   F   F
   8.74197479     9.56516854     0.15128437   F   F   F
   6.01966388     9.82202902     0.01690640   F   F   F
   3.06725685     9.80126422     0.20549987   F   F   F
   0.40278773     9.77259329     0.02542742   F   F   F
  10.56448727     4.02295977     0.01192203   F   F   F
   7.92010754     4.12304827     0.16511490   F   F   F
   4.97111215     4.19184685     0.00000000   F   F   F
   2.31916237     4.20561914     0.16624745   F   F   F
   6.23404552     8.55792240    10.93253011   T   T   T
   4.89352619     7.74528634    10.71096949   T   T   T
   5.30402220     8.64868648    10.61991632   T   T   T
   2.75150171     0.15624598     6.50310818   T   T   T
   1.24893493     1.38287535     4.48056795   T   T   T
   5.54834062     2.68192089     6.29001021   T   T   T
   2.74554158     2.70510055     6.33437548   T   T   T
```

5.54332884	0.23972226	6.44078464	T	T	T
4.24863925	1.37670076	4.48048451	T	T	T
8.36157342	0.15717578	6.46589812	T	T	T
6.85437575	1.38563928	4.48699384	T	T	T
11.15766778	2.68148780	6.29948681	T	T	T
8.35407735	2.71328686	6.29097339	T	T	T
11.17418621	0.23673909	6.44552295	T	T	T
9.86668378	1.37535143	4.48492172	T	T	T
2.70410290	5.70060352	6.30804746	T	T	T
1.20448321	7.01782883	4.48400038	T	T	T
5.50666084	8.15545854	6.50163223	T	T	T
2.69883742	8.26201586	6.45872758	T	T	T
5.51987698	5.71234779	6.28882193	T	T	T
4.21246401	7.03026552	4.49506825	T	T	T
8.32375665	5.65857100	6.29668606	T	T	T
6.80305308	7.01780950	4.48529659	T	T	T
11.11690785	8.14933984	6.42578475	T	T	T
8.30981037	8.21854109	6.41912380	T	T	T
11.11358409	5.70117309	6.29729109	T	T	T
9.81653584	6.99810877	4.47536494	T	T	T
4.20280171	9.80441154	4.58361938	T	T	T
5.54148634	2.89269985	2.53129684	T	T	T
4.11149030	4.21857828	0.46776477	F	F	F
2.65628555	11.04199769	2.63294632	T	T	T
5.47911305	11.09037536	2.59007382	T	T	T
1.21231262	4.19821023	4.40882913	T	T	T
2.74281357	2.94336522	2.60650709	T	T	T
1.36795485	4.19390193	0.46776477	F	F	F
4.25345756	4.19766534	4.41533634	T	T	T
11.15735162	2.89094387	2.53056395	T	T	T
9.72047525	4.21857828	0.46776477	F	F	F
8.26240414	11.02912388	2.64923488	T	T	T
11.08774260	11.08406099	2.58320886	T	T	T
6.79221695	4.20066189	4.38599831	T	T	T
8.34969996	2.93344488	2.62695349	T	T	T

6.97693979	4.19390193	0.46776477	F	F	F
9.88759316	4.18436930	4.39183727	T	T	T
5.48081211	8.52907093	2.59252965	T	T	T
4.02513034	9.82689836	0.46776477	F	F	F
2.74088443	5.46943217	2.60631949	T	T	T
5.52485911	5.51596778	2.52916376	T	T	T
1.15247141	9.81077649	4.58352791	T	T	T
2.66566168	8.57466365	2.62964942	T	T	T
1.28159488	9.80222201	0.46776477	F	F	F
9.81580279	9.80172459	4.58042105	T	T	T
11.08209326	8.51253704	2.57961812	T	T	T
9.63411529	9.82689836	0.46776477	F	F	F
8.33697461	5.43989407	2.63182277	T	T	T
11.15516617	5.49892661	2.54362404	T	T	T
6.75522581	9.80645964	4.60789829	T	T	T
8.27325778	8.56341856	2.61800031	T	T	T
6.89057983	9.80222201	0.46776477	F	F	F
1.37622193	1.46639326	0.46144125	F	F	F
9.74547659	1.28081934	0.51919325	F	F	F
6.98348978	1.42410103	0.45675783	F	F	F
4.13243805	1.30772896	0.51803158	F	F	F
4.05520408	7.10179356	0.50380377	F	F	F
6.89169239	7.02513194	0.44847630	F	F	F
9.65463868	6.91138193	0.52141773	F	F	F
1.28475020	6.94176239	0.45109260	F	F	F
2.73169125	4.19410608	5.37892610	T	T	T
4.10408190	1.45671106	6.45938450	T	T	T
1.39112618	1.45708895	6.45527514	T	T	T
8.34053599	4.18593640	5.26964233	T	T	T
9.73603868	1.45454432	6.44245537	T	T	T
6.97646799	1.45486627	6.45278671	T	T	T
2.67477493	9.84580729	5.55630451	T	T	T
4.06641599	6.91929949	6.43352199	T	T	T
1.32476623	6.92805874	6.44731373	T	T	T
8.29386577	9.80316117	5.55366422	T	T	T

9.69359709	6.93911685	6.43860819	T	T	T
6.95262866	6.92770366	6.42907151	T	T	T
5.58739500	1.40208006	1.43653272	F	F	F
2.75490012	1.38894091	3.39157279	T	T	T
5.47641484	11.17767544	4.50674352	T	T	T
1.39870638	4.21094306	2.28439975	T	T	T
4.07120685	4.20088303	2.23698967	T	T	T
5.52628013	2.81392281	4.41145807	T	T	T
11.19637995	1.40208006	1.43653272	F	F	F
8.36427350	1.37344337	3.40007654	T	T	T
11.08928437	11.17163658	4.49698151	T	T	T
6.99749387	4.19383294	2.27533346	T	T	T
9.69286485	4.18509907	2.25945442	T	T	T
11.16820824	2.81192688	4.41549899	T	T	T
5.50103503	7.01040014	1.43653272	F	F	F
8.31935662	7.00958835	3.38885956	T	T	T
5.51068667	5.57812255	4.40510749	T	T	T
1.31815973	9.80637257	2.26586904	T	T	T
4.01354298	9.81410537	2.28575640	T	T	T
5.49668264	8.44816300	4.49650034	T	T	T
11.11001998	7.01040014	1.43653272	F	F	F
2.70472608	7.01792904	3.39936314	T	T	T
11.14189331	5.57481013	4.41122335	T	T	T
6.93057835	9.80701049	2.25962469	T	T	T
9.61968594	9.80381481	2.25897407	T	T	T
11.10420182	8.43602267	4.50738987	T	T	T
11.02836321	11.07186140	8.56446976	T	T	T
1.31371939	2.17796338	8.98383750	T	T	T
0.01829131	4.20255305	7.86737940	T	T	T
4.03800166	6.15578943	8.93255159	T	T	T
1.27883125	6.22997441	8.96997841	T	T	T
2.63182222	8.56245591	8.74077190	T	T	T
4.17375929	2.19902637	9.00903909	T	T	T
6.91601599	2.14035957	9.00917439	T	T	T
5.44832026	4.18734118	7.83274059	T	T	T

6.87060658	6.22602416	8.97073158	T	T	T
5.47004787	8.51332691	8.52631615	T	T	T
5.48093894	11.09379679	8.57624635	T	T	T
8.26951087	11.07652363	8.99486608	T	T	T
9.76460115	2.13362725	8.99321687	T	T	T
8.33807528	4.19544805	8.23706672	T	T	T
9.73542163	6.27055826	8.99498503	T	T	T
8.28390794	8.52765137	8.98313235	T	T	T
11.03564246	8.55613092	8.62476995	T	T	T

Appendix 2. The POSCAR file for the products of H_2O dissociation at Pd_{18}(1+1) monolayer with two isolated vacancies deposited over γ-Al_2O_3(100) (Fig. 6c) optimized at the PBE-D3/PAW level.

```
18   O 65   Al 36   Pd 18
 1.000000000
   11.217970     0.000000     0.000000
   -0.086360    11.216740     0.000000
    0.000000     0.000000    24.572338
   18     65     36     18
Selective
Cartesian
   2.27168832     6.90904948     0.50404605  F   F   F
   9.57579524     5.95842863     0.22909170  F   F   F
   7.87798454     7.08746022     0.50403255  F   F   F
   4.01639974     8.01688421     0.12601133  F   F   F
   4.06826525     0.37052309     0.19062090  F   F   F
   2.36322847     1.52587412     0.50973860  F   F   F
   9.65286251     0.31583286     0.24970387  F   F   F
   7.97273005     1.47428835     0.50495137  F   F   F
   8.74197479     9.56516854     0.15128437  F   F   F
   6.01966388     9.82202902     0.01690640  F   F   F
   3.06725685     9.80126422     0.20549987  F   F   F
   0.40278773     9.77259329     0.02542742  F   F   F
  10.56448727     4.02295977     0.01192203  F   F   F
   7.92010754     4.12304827     0.16511490  F   F   F
   4.97111215     4.19184685     0.00000000  F   F   F
   2.31916237     4.20561914     0.16624745  F   F   F
   6.06912712     9.54544022    10.77019375 T   T   T
   5.22849571     6.81104672     9.66784928  T   T   T
   5.28018311     9.69539720    10.20778844 T   T   T
   2.75159331     0.15482005     6.51194115  T   T   T
   1.25072133     1.37905197     4.48614914  T   T   T
   5.54732463     2.68407239     6.29033561  T   T   T
   2.74465389     2.70397781     6.34075794  T   T   T
```

5.55716610 0.26015045 6.52708248 T T T
4.25617972 1.36467994 4.50431319 T T T
8.36874970 0.15807221 6.47695505 T T T
6.85100012 1.37609037 4.50779745 T T T
11.15975875 2.67851371 6.30109718 T T T
8.35948267 2.71674632 6.29121474 T T T
11.17581979 0.23460557 6.45188685 T T T
9.86645721 1.37163934 4.49050721 T T T
2.70726283 5.68912349 6.34820681 T T T
1.20984533 7.01230619 4.49660614 T T T
5.50133348 8.11061590 6.47353162 T T T
2.69552593 8.25221832 6.48473024 T T T
5.51780211 5.68673748 6.28615950 T T T
4.20073909 7.01690878 4.48918140 T T T
8.31582591 5.65924835 6.29391026 T T T
6.80462662 7.00893881 4.47948451 T T T
11.11023394 8.14378204 6.43503823 T T T
8.30290274 8.21412180 6.43698247 T T T
11.11209077 5.69518927 6.30273070 T T T
9.81619166 6.99735869 4.48069476 T T T
4.20736654 9.80381563 4.61690706 T T T
5.54054766 2.88653357 2.53582564 T T T
4.11149030 4.21857828 0.46776477 F F F
2.66012564 11.03892674 2.64031382 T T T
5.47885677 11.08859086 2.59955869 T T T
1.21561470 4.19798949 4.41607823 T T T
2.74469383 2.93571235 2.61278475 T T T
1.36795485 4.19390193 0.46776477 F F F
4.24958648 4.19256387 4.41731310 T T T
11.15859045 2.88959372 2.53396801 T T T
9.72047525 4.21857828 0.46776477 F F F
8.25987618 11.02668885 2.65608375 T T T
11.08846460 11.08138046 2.58779305 T T T
6.79151018 4.19267212 4.38343013 T T T
8.34901283 2.92784186 2.63222236 T T T

6.97693979	4.19390193	0.46776477	F	F	F
9.88951863	4.18287143	4.39353656	T	T	T
5.47936519	8.52993482	2.60226996	T	T	T
4.02513034	9.82689836	0.46776477	F	F	F
2.73828660	5.46383400	2.60377161	T	T	T
5.52398117	5.51099436	2.52750576	T	T	T
1.15390624	9.80536245	4.59778722	T	T	T
2.66666272	8.57523633	2.63358119	T	T	T
1.28159488	9.80222201	0.46776477	F	F	F
9.81577432	9.79797918	4.59123549	T	T	T
11.08350586	8.51075254	2.58477231	T	T	T
9.63411529	9.82689836	0.46776477	F	F	F
8.33833453	5.43550349	2.63341870	T	T	T
11.15639764	5.49870669	2.54696499	T	T	T
6.75213720	9.80771345	4.63354438	T	T	T
8.27229783	8.56380020	2.62298652	T	T	T
6.89057983	9.80222201	0.46776477	F	F	F
1.37622193	1.46639326	0.46144125	F	F	F
9.74547659	1.28081934	0.51919325	F	F	F
6.98348978	1.42410103	0.45675783	F	F	F
4.13243805	1.30772896	0.51803158	F	F	F
4.05520408	7.10179356	0.50380377	F	F	F
6.89169239	7.02513194	0.44847630	F	F	F
9.65463868	6.91138193	0.52141773	F	F	F
1.28475020	6.94176239	0.45109260	F	F	F
2.73222860	4.19174980	5.38835222	T	T	T
4.10112898	1.45867259	6.48821283	T	T	T
1.39184590	1.45419949	6.45991528	T	T	T
8.34074711	4.18815783	5.26646483	T	T	T
9.74380854	1.45661519	6.45013818	T	T	T
6.98686371	1.46575555	6.47204044	T	T	T
2.67261103	9.84001859	5.57752097	T	T	T
4.07186644	6.91283835	6.41500107	T	T	T
1.31777558	6.92106318	6.46732324	T	T	T
8.29561296	9.80068169	5.56566795	T	T	T

9.68862201	6.92890277	6.44403701	T	T	T
6.94115881	6.91429771	6.42996594	T	T	T
5.58739500	1.40208006	1.43653272	F	F	F
2.75933775	1.38320115	3.40473833	T	T	T
5.47795760	11.17205363	4.52262654	T	T	T
1.39888975	4.20602594	2.28361158	T	T	T
4.06964231	4.19682896	2.23596541	T	T	T
5.52365427	2.80930222	4.41431755	T	T	T
11.19637995	1.40208006	1.43653272	F	F	F
8.36257113	1.36957385	3.41025613	T	T	T
11.09048234	11.16769082	4.50404572	T	T	T
6.99779526	4.18989585	2.27612286	T	T	T
9.69361063	4.18268983	2.26027517	T	T	T
11.17010517	2.80995883	4.42030582	T	T	T
5.50103503	7.01040014	1.43653272	F	F	F
8.31945443	7.00655537	3.38892333	T	T	T
5.51109231	5.57140605	4.40187081	T	T	T
1.31913389	9.80602408	2.26496398	T	T	T
4.01573564	9.81263019	2.28354882	T	T	T
5.49682841	8.44040194	4.51469746	T	T	T
11.11001998	7.01040014	1.43653272	F	F	F
2.69983157	7.01365152	3.39366044	T	T	T
11.14416690	5.57249825	4.41579810	T	T	T
6.92882377	9.80554988	2.25877842	T	T	T
9.61943313	9.80306527	2.25921006	T	T	T
11.10501693	8.43296188	4.51462643	T	T	T
11.05947462	11.08182866	8.57762402	T	T	T
1.33926226	2.19300249	8.98323204	T	T	T
0.00054750	4.19716492	7.88462891	T	T	T
3.95600869	6.05087965	8.89356891	T	T	T
1.20844192	6.23321362	8.98710203	T	T	T
2.60379760	8.52865756	8.76346262	T	T	T
4.18674329	2.14637079	9.00470994	T	T	T
6.92995783	2.09344379	9.01678542	T	T	T
5.47338608	4.13836625	7.81096442	T	T	T

6.83046877	6.19467876	9.02940876	T	T	T
5.42410188	8.51295578	8.55194479	T	T	T
5.46846703	10.98723365	8.57120413	T	T	T
8.31519712	11.06201212	8.95115828	T	T	T
9.77173085	2.12472244	8.99776729	T	T	T
8.32273720	4.17006953	8.22406656	T	T	T
9.68479389	6.25795872	8.99993008	T	T	T
8.26108864	8.51473518	8.94869068	T	T	T
11.01251069	8.55870364	8.61934827	T	T	T